Performance Improvement for OFDM-RoF Transported 60 GHz System using Spatial Diversity and Multiplexing

Usman Habib[1], Anthony E Aighobahi[1], Manish Nair[1], Huiling Zhu[1], Terence Quinlan[2], Stuart D Walker[2] and Nathan J Gomes[1]

[1]Communication Research Group, University of Kent, Canterbury, UK

[2] School of Computer Science and Electronic Engineering, University of Essex, UK

uh23@kent.ac.uk

***Abstract*—60 GHz system architectures with Radio over Fiber (RoF) transport and integrated transmitters/receivers provide a comprehensive solution for future mobile systems. Since 60 GHz communication relies on line-of-sight (LoS) conditions and narrow-beam antennas to compensate the high path-loss, it has limitations in terms of coverage for multiple user locations. In this paper, performance analysis of a 60 GHz integrated transmitter and receiver system supported by RoF transport has been performed experimentally at different user locations for up to 1.5m transmission distance. Extension of experimental results to prove feasibility for longer distances has been shown with a simulation model, whose results at various shorter distances have been benchmarked against the acquired experimental results at different user locations. A modified version of the Saleh Valenzuela channel has been used to model the millimeter wave (mmW) LoS indoor experimental environment. Furthermore, as a proof of concept, we present an experimental analysis demonstrating an improvement in performance of the proposed RoF based 60 GHz system using spatial diversity and multiplexing. Channel measurements at different transmitter/receiver locations and their processing have shown that an improvement (decrease from 12.5% to 10.5%) in Error Vector Magnitude (EVM) can be achieved using the Alamouti Space Time Block Coding algorithm. Then it has been shown that a two-fold data rate increase can be obtained by combining data from two transmitter locations using the Zero Forcing algorithm.**

Keywords—Radio over Fiber, Remote Antenna Unit, Space Time Block Coding, Zero Forcing, Error Vector Magnitude

I. INTRODUCTION

The meteoric rise in demand for ever higher data-rates along with lower latencies has created new challenges in existing communication networks [1] which has led to research and development of fifth generation (5G) cellular networks. For new systems, the severe scarcity of spectrum in the current cellular bands has led to proposals for use of millimeter waves (mmW), where larger bands of frequency are available to offer high data rates, and in particular, the 60 GHz band, which has attracted substantial interest in recent research due to its unlicensed 7GHz bandwidth [2].

When adopting 60 GHz in indoor environments, the integration of mmW front end wireless links with Radio-over-fiber transmission is an attractive approach [3]. Properties of optical fiber communication such as ultra-high capacity and low loss propagation make it easy to realize a robust architecture for data transport between the Central Unit (CU) and the Remote Antenna Unit (RAU). The RoF part serves as a backbone for the whole network and provides centralized control [4]. RAU communication with the mobile user (MU) at 60 GHz can then be achieved using compact integrated transmitter and receiver units. Since 60 GHz wireless links rely on line-of-sight (LoS) conditions with narrow-beam antennas to compensate for the high path-loss [5], the coverage for multiple MU locations is still a challenge for 60 GHz communication systems that needs to be addressed, and has been highlighted in recent research [6]. Theoretical analysis has been presented for the indoor coverage of 60GHz systems [7] and the use of repeaters has been proposed to address the coverage issue [8]. However experimental implementations for 60 GHz transmission which show coverage improvement are lacking. Spatial diversity and spatial multiplexing techniques have been widely deployed in lower-frequency systems, such as IEEE 802.11n/ac and LTE 4G standards, to improve the reliability and/or increase the data rate of the system [9]. These can provide coverage improvement for a mmW communication system by making use of the decorrelation of different channel paths from spatially distributed transmitting units. We have previously shown that for a communication system based on photonic generation of a 25 GHz carrier, the use of Alamouti Space Time Block Coding STBC can provide improvement in Error Vector Magnitude (EVM) performance, while higher data rates through multiplexing can be achieved with the use of the Zero Forcing algorithm [10].

In this paper, a proof of concept to improve the performance of 60 GHz transmission to multiple user locations in indoor environments by using spatial diversity and spatial multiplexing is demonstrated by extending this previous work [10]. The experimental setup consists of OFDM-RoF transport and upconversion to 60 GHz using an integrated transmitter unit. Wireless transmission through 0.5m, 1m and 1.5m channels and performance analysis has been conducted at different user locations. The results have been extended to longer distances through simulations by modelling the experimental mmW environment. To perform theoretical analysis for mmW transmission systems, channel modeling at 60GHz has always been a challenge due to high path-loss and larger bandwidth; conventional channel models cannot be applied since they are

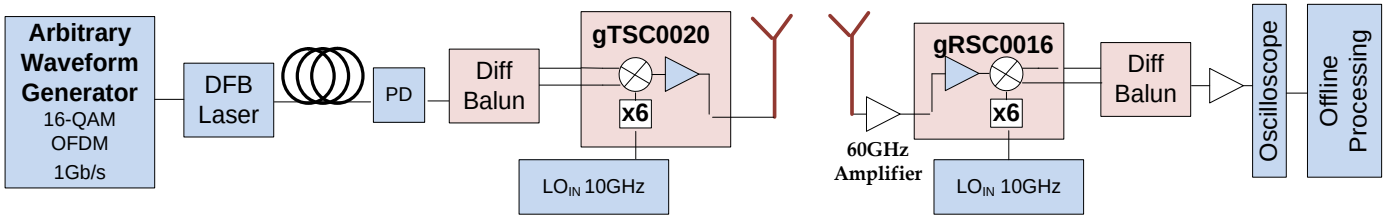

Fig. 1 System model for OFDM-RoF based 60GHz Transmission using Integrated Transmitter/Receiver

based on assumptions of narrow bandwidth. The propagation model presented here uses a modified Saleh Valenzuela (SV) [11] channel which accurately models a wide bandwidth channel and is used to analyze the system performance at longer distances. Furthermore, in order to experimentally analyze the performance of Alamouti STBC and Zero Forcing algorithms, the channel estimation at various transmitter and receiver locations is performed. To accomplish this, OFDM preambles (for channel estimation) and pilot tones (for phase tracking) were used to calculate channel coefficients for two transmitter positions and two receiver positions. From these experiments, it has been shown that performance at different user locations can be improved by reducing the EVM to below the threshold value (i.e. 12.5% for LTE) through spatial diversity using STBC processing. Moreover, it has also been demonstrated that multiple user data streams transmitted from different transmitter locations can be combined to obtain twice the data rate using spatial multiplexing through the Zero Forcing (ZF) algorithm.

The paper is organized as follows. Section II presents the experimental setup and its performance. The results have been extended for larger coverage areas using a simulation model in Section III. The geometrical arrangement of the experimental setup to achieve spatial diversity and multiplexing is explained in Section IV along with the results. The paper is concluded in Section V.

II. Experimental Setup

Fig. 1 shows the experimental setup in which a Distributed Feedback (DFB) Laser (Emcore 1935F) is modulated by an OFDM signal (at an IF of 1.5GHz and data rate of 1Gb/s) generated through a Tektronix 7122C Arbitrary Waveform Generator. The resultant signal is transmitted through a single mode optical fiber to the Central Unit CU where a photodiode (Appointech, 2.5Gbps InGaAs PIN, 0.7A/W) at the other end of the fiber converts the optically modulated signal to an IF signal at the RAU. The system parameters for the experiment can be summarized as in Table. I.

Table I: System Parameters for the experimental setup

Description	Unit	Value
Operating Frequency	GHz	60
OFDM Signal Bandwidth	MHz	305
Modulation	QAM	16
Tx Sampling Rate	GSps	12
Tx-Rx Separation	m	1.5
E_b/N_0 Tx SNR	dB	30

The IF signal from the photodiode is passed through a differential balun and DC blocker to be upconverted to 61.5 GHz using a gTSC0020 integrated transmitter with an LO of 10 GHz. The 61.5 GHz data modulated signal is transmitted over 1.5m wireless distance using an 18dBi gain horn antenna. At the other end, the mmW signal is received by a 16.8dBi slot antenna [12] and is downconverted to IF using a gRSC0016 integrated receiver using an LO of 10 GHz. The signal is captured using a Tektronix Digital Oscilloscope DPO72304DX for offline processing which includes carrier synchronization and demodulation for EVM analysis. Fig. 2 shows the performance of the experimental RoF transport from the central unit to RAU (without wireless transmission or 60 GHz upconversion) for different input IF power levels which indicates the input power levels for which optimum performance can be achieved through the initial RoF transport of the setup.

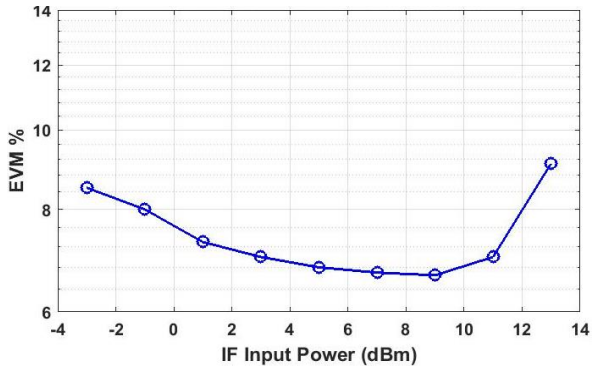

Fig. 2: Performance of RoF transport for different IF input power levels

The performance of the complete system including 60 GHz wireless transmission versus the power of the data signal from the photodiode after RoF transport is shown in Fig. 3. This

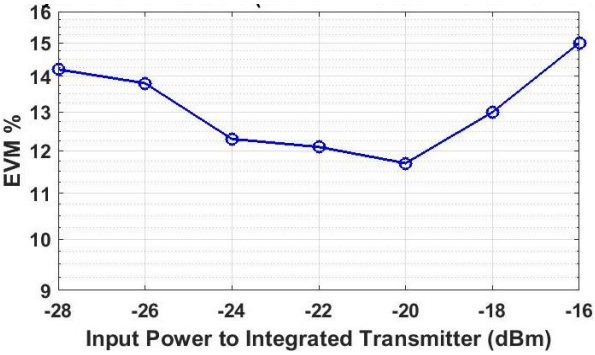

Fig. 3: System Performance of the RoF based 60 GHz Transmission for different IF power levels

shows that the EVM was found to be less than the 12.5% limit of LTE (for 16-QAM) for the overall system when the receiver was in LoS and in front of the transmitter as indicated by position C in geometric arrangement of the experimental setup in Fig. 4. Then, the measurements were performed for five receiver locations (A to E) as shown in Fig. 4 which correspond to angular locations of approximately -15° ,-7.5° ,0° ,7.5° and 15° from geometrical measurements. The transmission distance in the experimental analysis was constrained to 1.5m due to lack of availability of 60GHz band amplifier at the transmitter side.

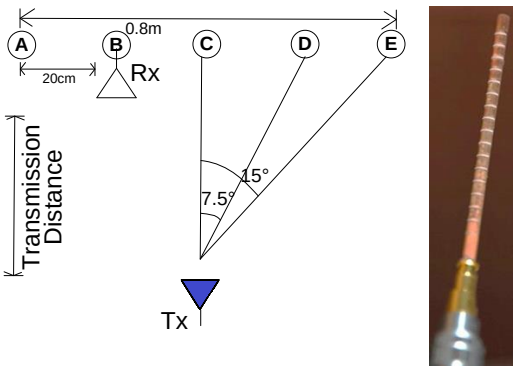

Fig. 4: Geometric orientation of the Experimental Setup and slot antenna array

A simulation model was developed based on the experimental results through the modelling of the 60GHz indoor experimental environment. The simulation results showed a high degree of agreement with the experimental results for multiple transmission distances of 0.7m, 1m and 1.5m and for the five receiver locations. Further simulations were performed to show the feasibility of the system for longer distances, which are presented in the next section.

III. Extension Of Experimental Results Using Wideband MMW Channel Model Simulations

In order to extend the experimental results of the 60 GHz transmission in the previous section to longer transmission distances, simulation of the indoor experimental environment by applying a LoS extension to the wideband modified Saleh Valenzuela (SV) channel impulse response (CIR) [13] has been considered. The modified SV channel model accurately represents wideband fading in terms of clustered multi-paths which is common in wideband mmW propagation environments, and hence has been chosen over other channel models, such as Rayleigh or Rician channel which are valid only for narrowband propagation [11,13]. Furthermore, other channel models such as WINNER 2, which have been previously used at mmW, are also narrowband and hence cannot be applied to our 305 MHz bandwidth system. Firstly, the coefficients of the wideband modified SV channel, for *v*-th cluster and *u*-th resolvable path of that cluster, are given by:

$$\alpha_l(t) = \sum_{v=0}^{V-1}\sum_{u=0}^{U-1}\sqrt{P_{uv}}\,\alpha_{uv}\,\delta(t-\tau_v-\tau_{uv})$$

$$= \sum_{l=0}^{L-1}\sqrt{P_l}\,\alpha_l\,\delta(t-l\tau) \qquad (1)$$

where α_l is the receiver CIR of the *l*-th resolvable multi-path signal component from the transmit antenna and $P_{l=uv}$ is the power of the *u-th* resolvable path in the *v-th* cluster. Here $1 \le l \le L$, where L is the total number of resolvable multi-path components, V denotes the number of clusters, U the number of resolvable paths in one cluster, and $L = UV$ is the total number of resolvable multi-paths at the receiver [14]. *l* is related to *u* and *v* by $l = vU + u$. In (1) $\alpha_{uv} = |\alpha_{uv}|e^{j\theta_{uv}}$ represents the fading of the *u*-th resolvable path in the *v*-th cluster connecting the transmit antenna to the receiver. τ_v is the time-of-arrival (ToA) of the *v*-th cluster and $\tau_{uv} = u\tau$ denotes the ToA of the *u*-th resolvable path in the *v*-th cluster. In our mmW channel, it is assumed that the average power of a multi-path at a given delay is related to the power of the first resolvable multi-path of the first cluster through the following relationship:

$$P_{uv}^k = P_{00}^k \exp(-\frac{T_v}{u})\exp(-\frac{T_{uv}}{u}) \qquad (2)$$

where $P_{uv,k} = P_l = |\alpha_{uv}|^2$ represents the expected power of the *u*-th resolvable path in the *v*-th multipath cluster connecting the user to the transmit antenna. Ψ and ψ are the corresponding power delay constants of the cluster and the resolvable multi-path respectively. For the channel model to be generic, we assume that the delay spread, which is $(L-1)\tau$ of the mmW channel spans $g \ge 1$ data bits, satisfying $(g-1)N_\tau \le (L-1)\tau \le gN_\tau$, where N_τ is the number of time slots per symbol. Secondly, we assume that the *L* resolvable multi-path components are randomly distributed and does not change over each symbol. Due to the wide bandwidth at mmW, all the *L* multi-path components can be resolved at the receiver (Rx) [14]. In the LoS extension for modeling directional antennas, it can be assumed that the first multi-path is the dominant component. A high rate of power decay in (2) will make all the other multi-path coefficients of the wideband SV channel close to zero. The parameters for generating the 3D mmW modified SV channel model at 60 GHz are given in Table II [15].

Table II: 3D mmW Modified SV Channel Parameters [15]

Description	Unit	Value
Inter-cluster inter-arrival rate	1/ns	0.21
Inra-cluster inter-arrival rate	1/ns	0.77
Inter-cluster decay factor	ns	4.19
Intra-cluster decay factor	ns	1.07
Small-scale fading RMS	dB	1.26
Inter-cluster Rician K-factor	dB	-10
Intra-cluster Rician K-factor	dB	-10

The comparison between experimental results and simulations is presented in Fig. 5 and shows agreement for various transmission distances and receiver locations which

demonstrates the accuracy of the modelling. Based on this observed agreement between the simulated and measured results, the EVM at various angular locations for longer transmission distances is shown in Fig. 6. The results were obtained by assuming 6dB amplification for 4.5m and 10dB amplification for 10m distance (with 2dB noise figure for both cases) of the transmit power . The simulation for 4.5m distance indicates the practicability of the system in rooms, and at 10m for larger transmission distances such as in shopping malls or airports where access points are usually installed on higher structures.

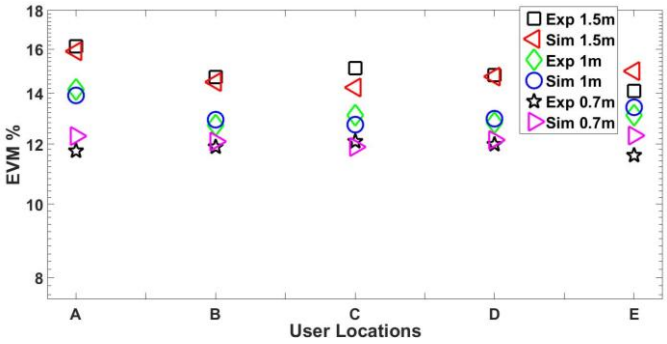

Fig. 5. EVM of simulated and experimental analysis at different angular locations of the user

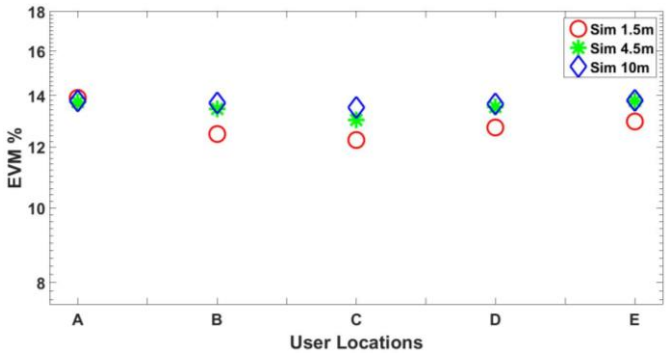

Fig. 6. Simulated EVMs at Different User Locations

From these results, the average spectral efficiency (in b/s/Hz) at 10m Tx-Rx separation distance has been calculated and plotted in Fig.7 at five user locations. In order to obtain the average spectral efficiency, the Rx SNR has been first calculated using

$$SNR_{Rx} = {(E_b/N_0 + SINR_i).C/B.K}\Big/{P_l} \qquad (3)$$

where the free space path loss P_l at 60GHz, given by

$$P_l = d.f_c.{4\pi}/{c} \sim 66\text{dB at } f_c = 60\text{GHz} \qquad (4)$$

In (3), E_b/N_o is the Tx SNR as mentioned in Table I, $SINR_i$ is the SINR of the i-th beam obtained from modelling the system along with the wideband mmW modified SV channel, C is the Tx sampling rate, B is the channel bandwidth (both are indicated in Table I), K=4 is the modulation index for 16QAM. In (4), d=*10m* is the Tx-Rx separation, fc=*60GHz* is the carrier frequency, and c is the velocity of light. Spectral efficiency is then calculated as:

$$SE = \log_2(1 + SNR_{Rx}) \qquad (5)$$

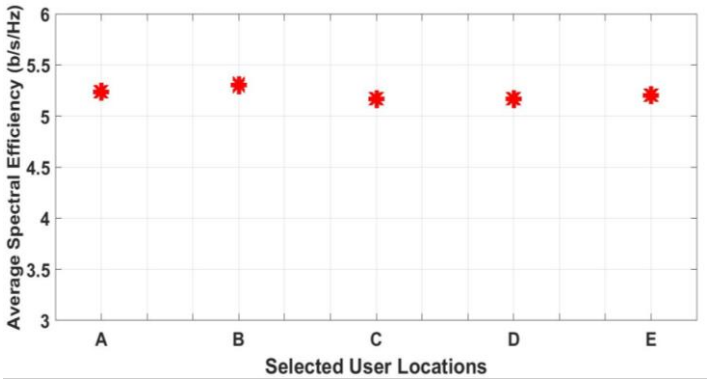

Fig. 7. Average Spectral Efficiency at selected user locations for Tx-Rx separation of 10m

The average spectral efficiency in Fig. 7 has been obtained over 15 simulation runs to characterize the effect of the randomized Additive White Gaussian Noise (AWGN). It can be observed in Fig. 7 that the average spectral efficiency obtained is just over 5 b/s/Hz, when the system parameters in Table I have been applied. The standard deviation was found to be 0.1 for the peak values of the spectral efficiency at these particular user locations.

IV. Experimental Achievement Of Spatial Diversity And Spatial Multiplexing

In this section, we demonstrate performance improvement at the previously discussed user locations and transmission distances through spatial diversity and spatial multiplexing. This can be achieved by measuring the channel transfer function for spatially distributed N transmit and M receive units and combining it with the transmitted symbols using STBC Alamouti or Zero Forcing algorithms. This arrangement can be represented as:

$$\begin{bmatrix} y_1 \\ y_2 \end{bmatrix} = \begin{bmatrix} h_{11} & h_{12} \\ h_{21} & h_{22} \end{bmatrix} \begin{bmatrix} x_1 \\ x_2 \end{bmatrix} + \begin{bmatrix} n_1 \\ n_2 \end{bmatrix} \qquad (6)$$

where y_1 and y_2 are the received OFDM symbols for Rx1 and Rx2, x_1 and x_2 are the transmitted symbols from Tx1 and Tx2, h_{11}, h_{21}, h_{12}, h_{22} are the measured channel transfer functions and n_1, n_2 represent the noise. In the first scenario, in order to achieve spatial diversity using the Alamouti STBC algorithm, the encoded signals are transmitted from two transmit locations over two symbol periods. The first period consists of two symbols x_1 and x_2, simultaneously transmitted, while during the second period, these symbols are transmitted again in the form of $-x_2^*$ from the first antenna and x_1^* from the second antenna. The Alamouti STBC decoder restores the transmitted symbol periods using (7) and (8):

$$x_1 = h_{11}y_1 + h_{12}y_2^* + h_{21}y_1 + h_{22}y_2^* \qquad (7)$$

$$x_2 = -h_{11}y_2^* + h_{12}^*y_1 - h_{22}y_2^* + h_{21}y_1^* \qquad (8)$$

where y_1 and y_2 are the received signals over two symbol periods and h_{11}, h_{21}, h_{12}, h_{22} represent the measured channel co-efficient estimated from the transmitted preamble symbols. In the second case, to achieve multiplexing gain using the zero-forcing algorithm, two different symbols x_1 and x_2 are simultaneously transmitted on two different antennas and the symbols are multiplexed using the zero-forcing algorithm. The zero-forcing algorithm uses (9) to restore the separate data where the weight matrix treats all transmitted signals as interference except for the desired signals from the target transmit antennas.

$$W_{ZF} = \left(H^H H\right)^{-1} H^H \tag{9}$$

The complex channel transfer matrix measurements can be obtained by placing transmit antennas at two distributed locations and capturing the data at two receiver location. In order to achieve improvement in performance, the channel transfer function matrix $\begin{bmatrix} h_{11} & h_{12} \\ h_{21} & h_{22} \end{bmatrix}$ was experimentally obtained by selecting two positions for the transmit antenna and marking them with a tape according to the layout shown in Fig 8. The coefficient h_{11} was measured by placing the transmit antenna in position Tx1 and receive antenna in position Rx1 while h_{12} was measured by moving the receive antenna to Rx2 (while keeping the transmit antenna at the same position of Tx1). Subsequently, to measure h_{21}, the transmit antenna was moved to Tx2 with receiving antenna at Rx1 and lastly, h_{22} was measured by moving the received antenna to Rx2 while keeping the transmit antenna at Tx2. These measurements were repeated for different user locations (A-E) over a span of 0.8m at wireless distance of 1.5m (Fig.8). The experiment was conducted for different separation of 20cm, 30cm and 40cm between Tx1 and Tx2 points as shown in Fig. 8.

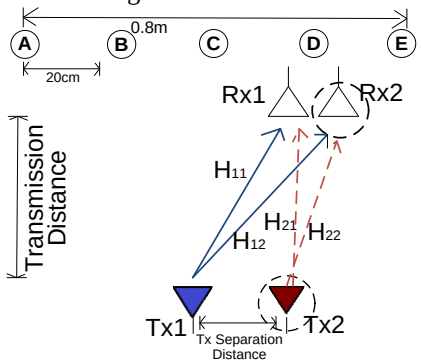

Fig. 8: Experimental Arrangement of Tx and Rx at Different Positions to achieve Spatial Diversity and Multiplexing

The values of h_{11}, h_{21}, h_{12}, h_{22} are used by (7) and (8) in MATLAB/Simulink software for offline processing using the Alamouti STBC algorithm. The EVM obtained at the five user locations (A to E) was improved using the STBC Alamouti signal processing algorithm for the received OFDM symbols (y_1 and y_2) as shown by the results in Fig. 9 where EVM for STBC processed output is less than SISO transmission and is under 12.5% (16-QAM limit for LTE) for each user location. STBC improves the transmission performance by making use of its orthogonal codes design and decorrelation of the received signals from multiple transmit locations. Thus, the achieved spatial diversity results in enhancement of coverage at multiple user locations.

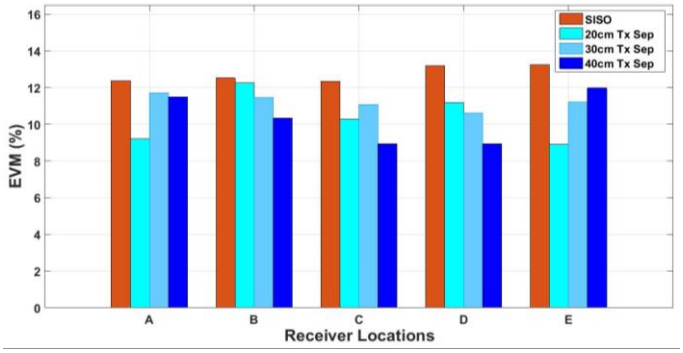

Fig. 9. SISO Demodulation versus STBC Alamouti Processing at Different User Locations

Additionally, the setup was used to realize multiplexing gains by combining the signals from two transmitter locations. One data stream with 0.5 Gb/s data rate is transmitted through location Tx1 in the first step and the data is captured at points Rx1 and Rx2 by moving the receiving antenna to the respective positions. Then, a second (different) data stream is transmitted through the same transmit antenna from location Tx2 and data was captured again at positions Rx1 and Rx2 as given by (9). The captured data is processed using the Zero Forcing algorithm to achieve an aggregate 1Gb/s data rate. Fig. 10 shows that the EVM of multiplexed data with combined data rate is under 12.5% EVM limit similar to the the single data stream. This verifies the achievement of multiplexing gain with the proposed system at 60GHz while keeping the spacing between points Tx1 and Tx2 as 20cm, 30cm and 40cm.

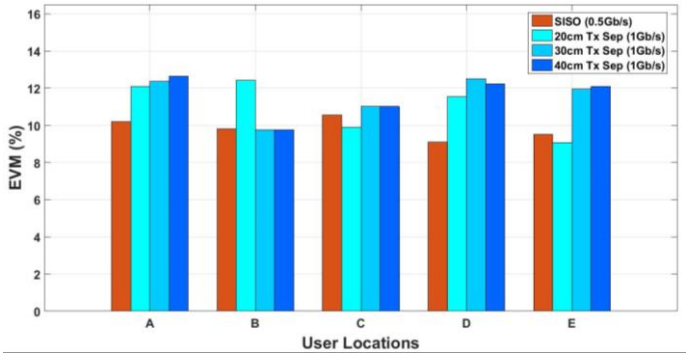

Fig. 10. SISO Demodulation (0.5Gb/s data rate) versus Zero Forcing Processing (with multiplexed data rate of 1Gb/s)

V. Conclusions

In this paper, the feasibility and analysis of an OFDM-RoF transported 60GHz system was presented and experimentally demonstrated for up to 1.5m transmission distance. A simulation model using a mmW modified SV channel was presented, that accurately modelled the 60 GHz experimental EVM results. The feasibility of the experimental setup for longer wireless distances was shown by extension of simulation results. Experimental results using offline processing, in order

to achieve improvement in performance and data rate, show that the channel estimation and use of the channel transfer function at different transmitter and receiver locations provided spatial diversity and multiplexing gain with Alamouti STBC and Zero-Forcing algorithms, respectively.

ACKNOWLEDGMENT

This work has been supported by the European Union's Horizon 2020 Research and Innovation programme under contract 643297 (RAPID), 644526 (iCIRRUS) and the UK Engineering and Physical Sciences Research Council's NIRVANA project (Reference No. EP/L026031/1).

REFERENCES

[1] M. Agiwal, A. Roy, N. Saxena, "Next generation 5G wireless networks: a comprehensive survey", in IEEE Communications Survays and Tutorials, Vol. 18 (3), 2016.

[2] S. Jiang, J. Peng, Z. Liu, J. Jiao, S. Jiang, "802.11ad Key Performance Analysis and Its Application in Home Wireless Entertainment", 17th IEEE Conference on Computational Science and Engineering CSE, 2014, pp. 1595-1598.

[3] M. Zhu, L. Zhang, J. Wang, L. Cheng, C. Liu, G. K. Chang, "Radio-over-fiber access architecture for integrated broadband wireless services", Journal of Lightwave Technology, 31(23), 2013, pp.3614-3620.

[4] L. Cheng et al. "Coordinated Multipoint Transmissions in Millimeter-Wave Radio-Over-Fiber Systems." Journal of Lightwave Technology, 34(2), 2016, pp.653-660.

[5] J. Guillory. et al, "Radio over fiber tunnel for 60 GHz wireless home network." In Optical Fiber Communication Conference, p. OWT6. Optical Society of America, 2011.

[6] P. Liu, M. D. Renzo, A. Springer, "Line-of-Sight Spatial Modulation for Indoor mmWave Communication at 60 GHz." IEEE Transactions on Wireless Communications 15 (11), 2016, pp.7373-7389.

[7] Y. Li, G. Wang, S. Li, F. Chen, Y. Liu, P. Wang, "Simulation and analysis of 60GHz millimeter-wave propagation characteristics in indoor complex environment.", IEEE International Conference on. Computational Electromagnetics (ICCEM), 2016, pp.278-280.

[8] J. Shen, D. Zhu, B. Li, P. Liang, "Repeater-enhanced millimeter-wave systems in multi-path environments." IEEE 26th Annual International Symposium on.Personal, Indoor, and Mobile Radio Communications (PIMRC), 2015, pp.769-774.

[9] IEEE 802.11-1999, IEEE Standard for Local and Metropoltian Area Networks – Wireless LAN Medium Access Control (MAC) and Physical Layer (PHY) Specifications, ISO/IEC 8802-11:1999 (E), 1999.

[10] U. Habib. U, A.E.Aighobahi, C.Wang, N.J.Gomes, "Radio over Fiber Transport of mm-Wave 2×2 MIMO for Spatial Diversity and Multiplexing", International topical meeting on Microwave Photonics (MWP), 2016, Long Beach CA, USA.

[11] O. E. Ayach, S. Rajagopal, S. Abu-Surra, Z. Pi, R. Heath, "Spatially Sparse Precoding in Millimeter Wave MIMO Systems", IEEE Transactions on Wireless Communications, vol. 13 (3) ,2014 , pp.1499-1513.

[12] T. Quinlan, S. Walker. "A 16.8 dBi quasi-discoidal radiation pattern antenna array for 60GHz non-line-of-sight applications.", Antennas and Propagation Conference (LAPC), 2014 Loughborough, 2014, pp.210-213.

[13] Q. Z. Ahmed, L. L. Yang, "Reduced-rank adaptive multiuser detection in hybrid direct-sequence time-hopping ultrawide bandwidth systems," IEEE Transactions on Wireless Communications, vol. 9 (1), 2010, pp. 156-167.

[14] A. Alkhateeb, R. W. Heath, "Frequency selective hybrid precoding for limited feedback millimeter wave systems", IEEE Transactions on Communications, vol. 64(5), 2016, pp. 1801-1818.

[15] H. Xu, V. Kukshya, T. Rappaport, "Spatial and Temporal Characteristics of 60-GHz Indoor Channels," IEEE Journal on Selected Areas in Communications, vol. 20,(3), 2002, pp. 620-630.